Eur. Phys. J. D **1**, 169-176 (1998)

THE EUROPEAN PHYSICAL JOURNAL D

Amplification of atomic L-R asymmetries by stimulated emission: experimental demonstration of sensitivity enhancement valuable for parity violation measurements

D. Chauvat, J. Guéna, Ph. Jacquier, M. Lintz, and M.A. Bouchiat[a]

Laboratoire Kastler Brossel[b], Département de Physique de l'École Normale Supérieure, 24 rue Lhomond, 75231 Paris Cedex 05, France

Received: 8 october 1997 / Accepted: 21 November 1997

Abstract. While all Atomic Parity Violation experiments on highly forbidden transitions in a Stark field have used the detection of fluorescence signals, our group is engaged in an experiment on the $6S - 7S$ cesium transition that uses a pump-probe scheme. The role of the probe beam is to detect the 7S state by stimulated emission. The detected Left-Right asymmetry (A_{LR}) appears directly on the transmitted probe beam and the technique relies on differential-mode atomic polarimetry. We present here experimental results which illustrate two essential features of this approach. First, A_{LR} is amplified when the optical thickness for the probe beam is increased, hence it is an increasing function of the Stark field. Secondly, the experimental sensitivity to A_{LR} is simultaneously increased, as demonstrated by our measurements of the signal-to-noise ratio. We emphasize also the advantage of choosing a probe transition that involves a "dark" state: the A_{LR} amplification is preserved at high levels of the probe intensity because saturation effects are greatly reduced.

PACS. 32.80.+a Other topics in atomic properties and interactions of atoms and ions with photons – 07.60.Fs Polarimeters and ellipsometers – 12.20.Fv Experimental tests

1 Introduction

For more than twenty years a continuous interest has been devoted to the study of Left-Right (L-R) asymmetries revealing the breaking of inversion symmetry in forbidden atomic transitions. Since the early seventies it has been recognized that their measurement in heavy atoms can provide an important test of the Standard Model [1]. From their very beginning [2,3] measurements of L-R asymmetries in cesium have reached an overall precision sufficient to provide quantitatively significant evidence of an electron-nucleon Z^0 exchange in a stable atom, at the level predicted by the Standard Model [4]. Today the remarkable precision of the measurements performed in cesium by the Boulder group [5] gives access to New Physics. This experimental activity has stimulated precise atomic theory calculations [6–8] and further progress in the calculations is expected. Today Atomic Parity Violation (APV) experiments remain pertinent to Particle Physics. For instance the unexpected events recently observed at the HERA collider [9] could be caused by new heavy (200 GeV/c^2) particles, called leptoquarks. These also contribute to the weak charge of the nucleus and it has been shown (see for instance [10]) that APV experiments provide significant constraints on such an interpretation. New APV measurements underway using a very different experimental approach, as described in the present article, are likely to reinforce the importance of such conclusions.

Considerable experimental efforts have been devoted to sensitivity enhancement in cesium and in other heavy elements at a number of laboratories. Up to now very different techniques have been employed. In experiments on highly forbidden transitions, like the $6S_{1/2} \rightarrow 7S_{1/2}$ transition in cesium [2,11] or the $6P_{1/2} \rightarrow 7P_{1/2}$ transition in thallium [12] the fluorescence light was detected, while in experiments involving allowed M_1 transitions in bismuth [13,14], lead [15] and thallium [16,17], the transmitted excitation beam is monitored. At present the thrust of experiments in highly forbidden transitions is towards developing more efficient means of detection. The recent Boulder experiment has succeeded in achieving an excellent signal-to-noise ratio. An optically pumped atomic beam is used and the $6S_{1/2} - 7S_{1/2}$ transition rate is detected with high efficiency via the modification induced in the final state of the 6S ground state population, but at the price of a certain loss in selectivity. A dilution of the asymmetry by a background on the transition rate and the overlap between adjacent Zeeman transitions require delicate (line shape dependent) corrections. Moreover in the control of

[a] e-mail: `marianne@physique.ens.fr`

[b] Laboratoire de l'Université Pierre et Marie Curie et de l'ENS, associé au CNRS (URA 18)

the systematic effects there are difficulties arising from the distortion of the line shape, which is modulated with the parameter reversals. As in all preceding experiments in highly forbidden transitions, the L-R asymmetry remains, within a factor close to unity, the ratio Im $E_1^{\rm pv}/\beta E$ where $E_1^{\rm pv}$ denotes the parity violating dipole amplitude of the $6S_{1/2} \rightarrow 7S_{1/2}$ transition and β the vector transition polarizability [1,18].

In the new approach followed at ENS, the L-R asymmetry is detected on a transmitted probe beam tuned to the allowed $7S_{1/2} \rightarrow 6P_{3/2}$ transition. This beam is amplified by stimulated emission, after excitation of the highly forbidden $6S_{1/2} \rightarrow 7S_{1/2}$ transition with an intense pulsed pump beam. The excited medium behaves like an anisotropic amplifier. Because of parity violation affecting the excitation process, the axes of anisotropy are not contained in the planes of symmetry of the experiment but are slightly tilted out of those planes [19,20]. The tilt angle $\theta^{\rm pv}$ is equal to $-$Im $E_1^{\rm pv}/\beta E$, the electroweak parameter to be measured. In this situation, detection by stimulated emission provides a large potential benefit, first, because of direct measurement of the electroweak L-R asymmetry without dilution and, second, thanks to the *amplification of this asymmetry*. In particular, as we show here, in contrast with all preceding experiments the measured asymmetry is an increasing function of the applied electric field.

A previous article [21] described theoretically in great detail the asymmetry amplification in the real conditions of our PV experiment. It was expected that such an effect could provide a real increase of the signal-to-noise ratio. However, one may have worried that light amplification generates noise, since the quantum state of the probe field is modified in the amplification process. In the actual experiment, there are also other sources of noise than quantum noise. Therefore, it was very important to verify experimentally the existence of the expected amplification of the asymmetry and to investigate simultaneously the behaviour of the Signal-to-Noise Ratio (SNR). Here we demonstrate experimentally the expected amplification, in quantitative agreement with the theory. In addition, we show that this amplification effectively results in *an improvement of the SNR*. This non-trivial result is of primary importance since it results in a net gain in sensitivity for precise PV measurements.

In Section 2 we shall rapidly outline the principle of our PV experiment, a pulsed pump-probe experiment using balanced mode polarimetry, and we summarize the main conclusions of the previous theoretical paper [21] which is used as a guide for our experimental investigations. Section 3 contains the experimental verification of the L-R asymmetry amplification. Since the PV asymmetry is very small ($\theta^{\rm pv} \approx 10^{-6}$ rad), we have performed the measurements by using the L-R asymmetry induced by a Faraday rotator serving as a calibration device for the PV experiment. This much larger parity conserving signal has optical properties exactly similar to the PV effect. In Section 4, we discuss the effective SNR improvement associated with the asymmetry amplification. The key point here lies in the experimental procedure retained to measure the asymmetry: in balanced mode operation the variance of the asymmetry is always $1/N$ where N is the average number of detected photons, *whatever the quantum state of the amplified light field*. Our results demonstrate unambiguously the increase of the SNR with light amplification. This improvement of the SNR is characterized by the decrease of the "noise equivalent angle" or NEA, defined as the angle equal to the noise. In conclusion (Sect. 5) we summarize various ways of improving the sensitivity to the electroweak L-R asymmetry in our PV experiment made possible by a better understanding of its particular features.

2 Principle of A_{LR} amplification. Summary of the theoretical analysis

Our experiment follows a pump-probe scheme using two pulsed linearly polarized laser beams resonant with the hyperfine components of the highly forbidden $6S_{1/2}, F_1 \rightarrow 7S_{1/2}, F_2$ (pump) and allowed $7S_{1/2}, F_2 \rightarrow 6P_{3/2}, F_3$ (probe) transitions of the cesium atom. It is during the pulsed excitation of the highly forbidden transition that a manifestation of PV occurs. An electric field $\mathbf{E}$ is applied parallel to the excitation beam wavevector which allows one to perform an optimization of the transition rate in order to obtain the best sensitivity to the PV effect. The large population of $7S_{1/2}, F_2$ atoms thus produced is detected through the subsequent transient gain which appears at the $7S_{1/2}, F_2 \rightarrow 6P_{3/2}, F_3$ frequency, by stimulated emission of the collinear probe laser beam. The excitation by the linearly polarized pump beam endows the vapour with a parity conserving linear dichroism whose optical axes are parallel and perpendicular to the polarization $\hat{\boldsymbol{\epsilon}}_{\rm ex}$ of the beam. PV manifests itself as a modification of those optical axes which deviate from the previous ones by a tiny angle ($\approx 10^{-6}$ rad) *whose sign reverses with the direction of* $\mathbf{E}$. This effect can be described as a small, $\mathbf{E}$-odd, linear dichroism for the probe with axes at 45° to $\hat{\boldsymbol{\epsilon}}_{\rm ex}$ in addition to the main, parity conserving, linear dichroism. The incoming probe polarization $\hat{\boldsymbol{\epsilon}}_{\rm pr}$ is set either parallel or orthogonal to $\hat{\boldsymbol{\epsilon}}_{\rm ex}$ and the outgoing polarization is analyzed using a balanced polarimeter [22–24].

2.1 Simple presentation, using two refractive indices

For times short compared to the $7S_{1/2}$ lifetime the vapor behaves as an anisotropic amplifier characterized by two principal axes with respective amplification coefficients of the field per unit length, $\alpha_\perp$ and $\alpha_\parallel$, identified with the imaginary parts of the refractive indices $n_\perp$ and $n_\parallel$. If we define

$$\alpha = \frac{\omega_0}{2\epsilon_0 c\gamma\hbar}|{\rm d}(7S_{1/2,F_2}; 6P_{3/2,F_3})|^2\,\mathcal{N}_{7S,F_2}\,c(F_1, F_2, F_3) \tag{1}$$

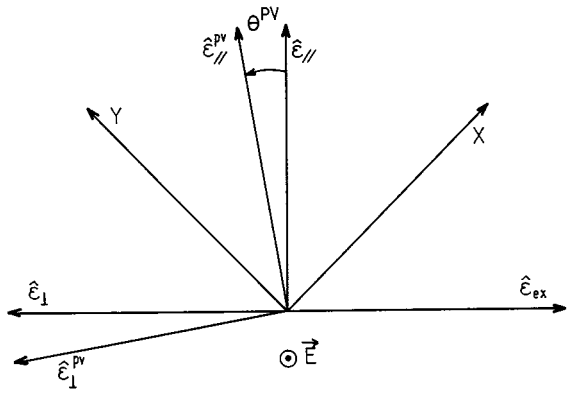

Fig. 1. Main axes of the experimental configuration: $\hat{\boldsymbol{\epsilon}}_{\rm ex}$: excitation polarization; $\hat{\boldsymbol{\epsilon}}_{\parallel}$, $\hat{\boldsymbol{\epsilon}}_{\perp}$: optical axes without PV effect; $\hat{\boldsymbol{\epsilon}}_{\parallel}^{\rm pv}$, $\hat{\boldsymbol{\epsilon}}_{\perp}^{\rm pv}$: optical axes with PV effect. For calibration $\theta^{\rm pv}$ is replaced by $\theta^{\rm pv} \pm \theta^{\rm cal}$.

then, $\alpha_{\perp}$ and $\alpha_{\parallel}$ differ by the $c(\mathrm{F}_1, \mathrm{F}_2, \mathrm{F}_3)$ coefficient involving Clebsch-Gordan coefficients and the magnetic quantum number probability distribution of the excited $7\mathrm{S}, \mathrm{F}_2$ state prepared with $\hat{\boldsymbol{\epsilon}}_{\rm ex}$ set either parallel or orthogonal to $\hat{\boldsymbol{\epsilon}}_{\rm pr}$ [21]. The other parameters involved are the square of the dipole matrix element of the probe transition $|\mathrm{d}(7\mathrm{S}_{1/2,\mathrm{F}_2}; 6\mathrm{P}_{3/2,\mathrm{F}_3})|^2$, the number density of atoms excited by the pump beam $\mathcal{N}_{7\mathrm{S},\mathrm{F}_2}$, proportional to E^2, and the damping rate $\gamma = T_2^{-1}$ of the optical dipole at the probe frequency $\omega_0/2\pi$.

For symmetry reasons, without parity violation the eigendirections for the probe polarization $\hat{\boldsymbol{\epsilon}}_{\rm pr}^{\rm in}$ would be: $\hat{\boldsymbol{\epsilon}}_{\parallel} = \frac{\mathbf{E}}{E} \times \hat{\boldsymbol{\epsilon}}_{\rm ex}$ and $\hat{\boldsymbol{\epsilon}}_{\perp} = \frac{\mathbf{E}}{E} \times \hat{\boldsymbol{\epsilon}}_{\parallel}$. Due to parity violation, the eigendirections are tilted (see Fig. 1) by a small angle:

$$\theta^{\rm pv} = -\mathrm{Im}\, E_1^{\rm pv}/\beta E\,.$$

The eigen axes of the amplifying medium are therefore:

$$\hat{\boldsymbol{\epsilon}}_{\parallel}^{\rm pv} = \hat{\boldsymbol{\epsilon}}_{\parallel} + \theta^{\rm pv}\hat{\boldsymbol{\epsilon}}_{\perp} \text{ and } \hat{\boldsymbol{\epsilon}}_{\perp}^{\rm pv} = \hat{\boldsymbol{\epsilon}}_{\perp} - \theta^{\rm pv}\hat{\boldsymbol{\epsilon}}_{\parallel}.$$

If the probe beam enters the amplifying medium with its polarization along $\hat{\boldsymbol{\epsilon}}_{\parallel}$, at the output it acquires a polarization component along $\hat{\boldsymbol{\epsilon}}_{\perp}$, namely $\mathbf{E}_{\rm out}{=}\mathcal{E}_{\rm in}[\hat{\boldsymbol{\epsilon}}_{\parallel} \exp(\alpha_{\parallel}L) + \theta^{\rm pv}\,\hat{\boldsymbol{\epsilon}}_{\perp}(\exp(\alpha_{\parallel}L) - \exp(\alpha_{\perp}L))]$ where L is the length of the amplifying column. $\mathbf{E}_{\rm out}$ is analyzed with a two-channel balanced polarimeter whose fixed principal axes $\hat{\mathbf{X}}$ and $\hat{\mathbf{Y}}$ are oriented at $\pm 45^{\rm o}$ to $\hat{\boldsymbol{\epsilon}}_{\rm pr}^{\rm in}$. Both signals $S_{\rm X}$ and $S_{\rm Y}$ associated with either one of the two channels X and Y are measured at each laser shot, thus providing a determination of the L-R asymmetry:

$$A_{\rm LR} \equiv \frac{S_{\rm Y} - S_{\rm X}}{S_{\rm Y} + S_{\rm X}} = -2\theta^{\rm pv}\left(\exp\left(\mathcal{A}_{\parallel}\left(\frac{\alpha_{\perp} - \alpha_{\parallel}}{2\alpha_{\parallel}}\right)\right) - 1\right) \tag{2}$$

$\mathcal{A}_{\parallel} \equiv \ln(I_{\rm pr}^{\rm out}/I_{\rm pr}^{\rm in})$ is the optical density for the probe field when it is polarized along $\hat{\boldsymbol{\epsilon}}_{\parallel}$, with $I_{\rm pr}^{\rm in}$ and $I_{\rm pr}^{\rm out}$ denoting the ingoing and outgoing intensities of the probe beam. A crucial parameter appearing in equation (2) is the optical anisotropy of the excited medium $\eta = \left(\alpha_{\perp} - \alpha_{\parallel}\right)/2\alpha_{\parallel}$ which depends only on the hyperfine quantum numbers $(\mathrm{F}_1, \mathrm{F}_2, \mathrm{F}_3)$ of the atomic states. The choice $(3, 4, 4)$, with the largest anisotropy $\eta = \frac{11}{12}$, leads to the most favorable situation. Note that to derive equation (2) we made use of the relation $\mathcal{A}_{\parallel} = 2\alpha_{\parallel} L$, characteristic of "linear amplification", but its validity does not extend beyond the present complex index model.

It may be useful here to underline that the parity-conserving transition dipole for the excitation transition in a longitudinal electric field, is directed along $\frac{\mathbf{E}}{E} \times \hat{\boldsymbol{\epsilon}}_{\rm ex}$, hence perpendicular to $\hat{\boldsymbol{\epsilon}}_{\rm ex}$. Therefore, one should bear in mind that the configuration with the pump and probe *dipoles quasi parallel* (optical thickness denoted $\mathcal{A}_{\parallel}$) corresponds to incident pump and probe *polarizations perpendicular*.

2.2 Realistic situation with a low probe intensity

The description of the amplification process in terms of complex indices is only valid in well defined conditions not actually satisfied by the experiment. The detailed analysis performed in reference [21] uses a semiclassical method. The problem has been solved for an anisotropic medium in full generality, *i.e.* with no restriction concerning the duration of the probe pulse $t_{\rm p}$ compared to T_2 and to the $7\mathrm{S}_{1/2}$ state lifetime $T_{7\mathrm{S}} = 48$ ns. It is found that as long as $\mathcal{A} \lesssim 1$ the dependence of $A_{\rm LR}$ *versus* $\mathcal{A}$ corresponding to equation (2) is practically unmodified. By contrast, the variation of $\mathcal{A}$ *versus* αL is only approximately linear and its slope has to be renormalized by a factor 0.6, for the ratio $t_{\rm p}/T_2 = 1.43$, corresponding to our experiment. The results of the complex index model are recovered in the limit $T_2 \ll t_{\rm p} \ll T_{7\mathrm{S}}$.

From explicit computations [21] and for the realistic values $T_2 = 14$ ns and $t_{\rm p} = 20$ ns, the calculated values of $A_{\rm LR}$ over the intervals of $\mathcal{A}$ covered experimentally turn out to be well fitted by the following expressions:

$$\hat{\boldsymbol{\epsilon}}_{\rm pr}^{\rm in} = \hat{\boldsymbol{\epsilon}}_{\parallel}\colon\ A_{\rm LR}^{\parallel} = -\theta^{\rm pv} C_{\parallel}\left[\exp\left(\mathcal{A}_{\parallel}\left(\frac{\alpha_{\perp} - \alpha_{\parallel}}{2\alpha_{\parallel}}\right)\right) - 1\right] \quad \text{with } C_{\parallel} = 2.0 \tag{3}$$

$$\hat{\boldsymbol{\epsilon}}_{\rm pr}^{\rm in} = \hat{\boldsymbol{\epsilon}}_{\perp}\colon\ A_{\rm LR}^{\perp} = -\theta^{\rm pv} C_{\perp}\left[1 - \exp\left(\mathcal{A}_{\perp}\left(\frac{\alpha_{\parallel} - \alpha_{\perp}}{2\alpha_{\perp}}\right)\right)\right] \quad \text{with } C_{\perp} = 2.26 \tag{4}$$

where it must be remembered that the relation between $\mathcal{A}$ and α is no longer straightforward.

Both equations predict an increase in the magnitude of $A_{\rm LR}$ *versus* $\mathcal{A}$. The attractive feature of this amplification mechanism lies in the fact that it occurs simultaneously with an amplification of the signal intensity. Such a characteristic is unusual, since, in all PV Stark experiments based on detection of spontaneous emission, $A_{\rm LR}$ is, up to a numerical factor close to 1, equal to $\theta^{\rm pv} = -\mathrm{Im}\, E_1^{\rm pv}/\beta E$, so that a reduction of E which increases the asymmetry leads to an unavoidable loss of the fluorescence signal proportional to $\beta^2 E^2$. Here by contrast it is advantageous to increase E for it increases both the signal $I_{\rm pr}^{\rm out}$ *and* the asymmetry $A_{\rm LR}$. Since $\alpha_{\perp}$ and $\alpha_{\parallel}$ are proportional to E^2

we see that $A_{\rm LR}$ first grows linearly with E whatever the relative orientation of $\hat{\boldsymbol{\epsilon}}_{\rm in}^{pr}$ and $\hat{\boldsymbol{\epsilon}}_{\rm ex}$, and then much faster, as $\left(\exp\left(KE^2\right)-1\right)/E$, in the most favorable configuration, $\hat{\boldsymbol{\epsilon}}_{\rm pr}^{\rm in} \perp \hat{\boldsymbol{\epsilon}}_{\rm ex}$. Such a result is of considerable value in the optimization process of the signal-to-noise ratio.

2.3 Influence of the probe saturation

At low probe intensities, increasing the intensity seems *a priori* advantageous since it reduces the statistical photon noise on the asymmetry. Only saturation effects may in principle limit the value of $I_{\rm pr}$ not to be exceeded. The problem of saturation has not been treated in full generality, though in reference [21] it is solved in cases of special interest, *i.e.* those of the $6S_{1/2,F\pm1} \rightarrow 7S_{1/2,F} \rightarrow 6P_{3/2,F}$ transitions, with $\hat{\boldsymbol{\epsilon}}_{\rm pr}^{\rm in} \perp \hat{\boldsymbol{\epsilon}}_{\rm ex}$, which are characterized by the largest anisotropy and hence the largest L-R asymmetry amplification. Let us choose the quantization axis along the eigen axis of the vapor $\hat{\boldsymbol{\epsilon}}_{\parallel}^{\rm pv}$. The probe field can be decomposed into a large component parallel to this axis and a very small one, along the perpendicular direction. The large component perturbs the population difference between upper and lower substates having equal magnetic quantum numbers. Its treatment involves the resolution of an integro-differential equation which has been performed analytically. The small component (proportional to $\theta^{\rm pv}$) is sufficiently weak not to affect the upper state density matrix. Therefore the propagation of the small component can be treated in the low intensity limit using the time-dependent population differences imposed by the large component. The remarkable feature of the situation we have retained is that the $|7S_{1/2}, F_2, m_F = 0\rangle$ substate, which is the most populated by the pump, is not coupled to the large component of the probe radiation field ("dark state"). It is quite understandable that, in such conditions, saturation by the probe beam is considerably slowed down. At the same time asymmetry amplification still takes place at large saturation of the field amplification, since the small component is coupled to all the states and particularly strongly to the most populated one. This mechanism is illustrated in a particularly simple and clear situation corresponding to a pump-probe transition $6S_{1/2}, F = 0 \rightarrow 7S_{1/2}, F = 1 \rightarrow 6P_{3/2}, F = 1$, (which is actually relevant to a few Cs radioactive isotopes of nuclear spin 1/2), as shown in Figure 2a. With our choice of quantization axis the pump beam excites $\Delta m_F = 0$ transitions only: therefore there is a single populated substate, $|7S_{1/2}, F = 1, m_F = 0\rangle$. The probe field is decomposed as just indicated: the large component parallel to the quantization axis, which can only connect states with identical value of m_F cannot interact with the dark state $m_F = 0$, since the $\Delta F = 0, 0 \rightarrow 0$ transition is forbidden. By contrast the small component, proportional to the tilt angle, interacts with the atoms in the $m_F = 0$ substate and is therefore amplified. In this extreme situation the probe intensity is not amplified while the asymmetry is. This example sheds light on a paradoxical feature of the mechanism of $A_{\rm LR}$ amplification: the configuration with the smallest probe amplification provides the largest asymmetry amplification. Even in the case where all atoms are concentrated in a dark state and the amplification of the probe intensity vanishes, an amplification of the asymmetry remains.

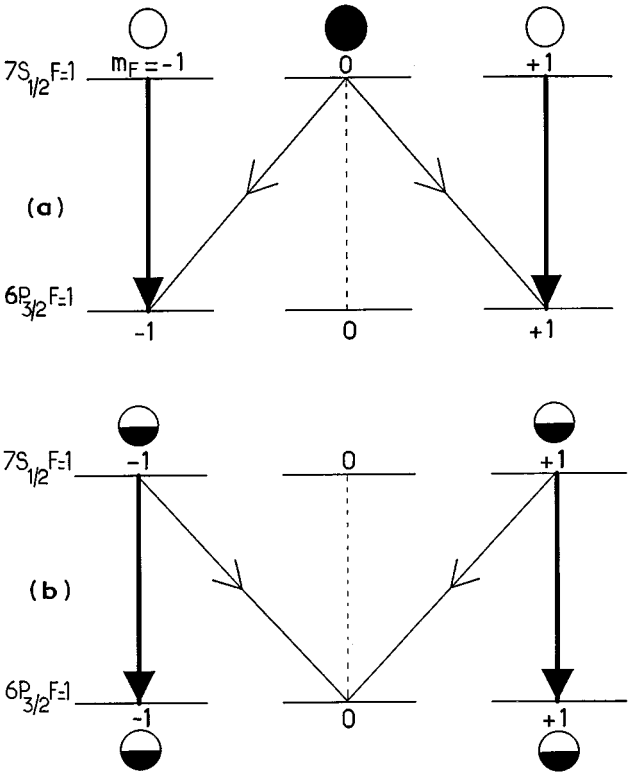

Fig. 2. (a) Asymmetry amplification for a $6S_{1/2}, F = 0 \rightarrow 7S_{1/2}, F = 1 \rightarrow 6P_{3/2}, F = 1$ pump-probe transition, when $\hat{\boldsymbol{\epsilon}}_{\rm pr}^{\rm in} \perp \hat{\boldsymbol{\epsilon}}_{\rm ex}$. With the quantization axis chosen along $\hat{\boldsymbol{\epsilon}}_{\parallel}^{\rm pv}$, the single state populated by the pump is $|F = 1, m_F = 0\rangle$. Without parity violation, the probe can only induce $\Delta m_F = 0$ transitions, whose probability cancels for the $m_F = 0$ substate. However, because of the PV tilt of the eigenaxes, the probe field has also a small component able to induce $\Delta m_F = \pm 1$ transitions starting from the singly populated substate, so that the L-R asymmetry is amplified. (b) Asymmetry amplification for the same transition in the case $\hat{\boldsymbol{\epsilon}}_{\rm pr}^{\rm in} \perp \hat{\boldsymbol{\epsilon}}_{\rm ex}$. The quantization axis being now chosen along $\hat{\boldsymbol{\epsilon}}_{\perp}^{\rm pv}$, the upper state is prepared with equal populations in both $|m_F| = 1$ states. Asymmetry amplification can still take place (see Sect. 2.3).

Explicit calculations for natural Cs ($I = 7/2$) predict that saturation of the probe transition by the optical field should provide manifestation of the asymmetry amplification at lower optical densities and, notwithstanding, at larger fluxes of *transmitted* photons (see Fig. 5 in [21]).

One may also wonder what happens concerning saturation in the other polarization configuration, $\hat{\boldsymbol{\epsilon}}_{\rm ex} \parallel \hat{\boldsymbol{\epsilon}}_{\rm pr}^{\rm in}$. Asymmetry amplification for the simple $6S_{1/2}, F = 0 \rightarrow 7S_{1/2}, F = 1 \rightarrow 6P_{3/2}, F = 1$ transition, when the excitation and probe dipoles are nearly perpendicular, is illustrated in Figure 2b. The quantization axis being now chosen along $\hat{\boldsymbol{\epsilon}}_{\perp}^{\rm pv}$, the upper state is prepared with equal populations in both $|m_F| = 1$ states. A saturating probe

beam equalizes the populations between the initial and final $|m_F| = 1$ states. Nevertheless, a certain gain remains for the small component of the probe which induces the $\Delta m_F = \pm 1$ transitions, so that the L-R asymmetry still increases with $\mathcal{A}$. We may note, however, that in this case a rapid redistribution among the $6P_{3/2}, m_F$ populations due to 6S-6P exchange collisions can reduce the magnitude of the effect.

3 Experimental demonstration of A_{LR} amplification at increasing optical densities

3.1 Electroweak and calibration asymmetries

The picture of the PV effect as a tiny rotation of the optical axes of the vapour dichroism suggests a straightforward way to calibrate θ^{pv}. With a Faraday rotator placed in the excitation beam path we purposely rotate the excitation polarization $\hat{\boldsymbol{\epsilon}}_{ex}$ by an angle θ^{cal} known to at least one per cent accuracy, while $\hat{\boldsymbol{\epsilon}}^{in}_{pr}$ remains unaltered [20,24]. Consequently the L-R asymmetry $(S_Y - S_X)/(S_Y + S_X)$ acquires a parity conserving contribution. The angle θ^{cal} being of the order of 10^{-3} rad, a lowest-order treatment is valid and equation (2) becomes:

$$A_{LR}\left(\theta^{cal}, \mathbf{E}\right) = -\left(\theta^{cal} + \theta^{pv}\right) C_{\parallel} \left[\exp\left(\mathcal{A}_{\parallel}\eta\right) - 1\right] . \quad (5)$$

The reversal of θ^{cal} allows extraction of the calibration signal since:

$$A^{cal}_{LR} = \frac{1}{2}\left(A_{LR}\left(+\theta^{cal}, \mathbf{E}\right) - A_{LR}\left(-\theta^{cal}, \mathbf{E}\right)\right) \quad (6)$$

$$= -\theta^{cal} C_{\parallel} \left[\exp\left(\mathcal{A}_{\parallel}\eta\right) - 1\right] . \quad (7)$$

This signal is very well defined for short integration times and bears the same amplification as the PV effect (Eqs. (3) and (4)). Experimentally, we observe an excellent proportionality of A^{cal}_{LR} to θ^{cal} in the explored range (10^{-4} to 10^{-2} rad).

One way to reconstruct the PV signal consists in reversing alternatively θ^{cal} and the electric field:

$$A^{pv}_{LR} = \frac{1}{2}\left[A_{LR}\left(\theta^{cal}, +\mathbf{E}\right) - A_{LR}\left(\theta^{cal}, -\mathbf{E}\right)\right] \quad (8)$$

$$= -\theta^{pv} C_{\parallel} \left[\exp\left(\mathcal{A}_{\parallel}\eta\right) - 1\right] . \quad (9)$$

The PV angle is then deduced by a simple proportionality relation:

$$\theta^{pv} = \theta^{cal}\, A^{pv}_{LR}/A^{cal}_{LR} . \quad (10)$$

In fact, the reconstitution of θ^{pv} involves other differential and normalization procedures taking into account additional reversals [24]. It ensures that both the PV and the calibration signals are free from spurious effects such as "geometrical" ones, due to the possible alteration of the amplified probe beam geometry, or electromagnetic interferences for instance [23].

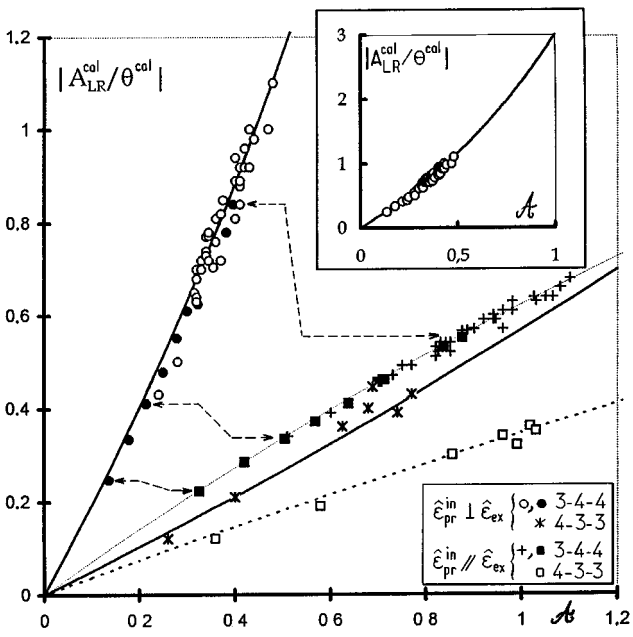

Fig. 3. L-R asymmetry as a function of the optical density $\mathcal{A}$ for two hfs transitions and for both $\hat{\boldsymbol{\epsilon}}^{in}_{pr} \parallel \hat{\boldsymbol{\epsilon}}_{ex}$ and $\hat{\boldsymbol{\epsilon}}^{in}_{pr} \perp \hat{\boldsymbol{\epsilon}}_{ex}$ configurations. Dotted arrows join examples of points obtained in otherwise identical conditions. Black and open circles respectively correspond to variations of $\mathcal{A}$ induced by varying E (from 1.2 kV/cm to 2.2 kV/cm) and the pump energy (from 1.5 to 2 mJ). Probe delay 6 ns; constant probe saturation ($\sim 4 \times 10^7$ photons per reference probe pulse); calibration tilt = 1.2 or 1.7 mrad. Inset: extrapolation for the $6S_{1/2}, F = 3 \rightarrow 7S_{1/2}, F = 4 \rightarrow 6P_{3/2}, F = 4$ transition and $\hat{\boldsymbol{\epsilon}}^{in}_{pr} \perp \hat{\boldsymbol{\epsilon}}_{ex}$.

3.2 Experimental results

Figure 3 summarizes the results obtained for two hfs pump-probe transitions $(3,4,4)$ and $(4,3,3)$ whose respective anisotropy parameters are 11/12 and 3/4. In both cases $A^{cal}_{LR}/\theta^{cal}$ is plotted as a function of the optical density of the excited medium and compared to the theoretical predictions. The optical density is obtained by comparison of the *amplified* probe pulse to a *reference* probe pulse sent 1 ms later when all cesium atoms have decayed [23]: hence $\mathcal{A} = \ln((S_X + S_Y)^{amp}/(S_X + S_Y)^{ref})$. The case of the $(3,4,4)$ transition is the most significant in view of its large anisotropy parameter. The solid and dotted curves represent the theoretical predictions *without any adjusted parameter*. They appear in excellent agreement with the experimental points for both transitions.

Figure 3 exhibits the most interesting feature of this work for $\hat{\boldsymbol{\epsilon}}^{in}_{pr} \perp \hat{\boldsymbol{\epsilon}}_{ex}$. Indeed an increase of $\mathcal{A}_{\parallel}$ not only increases exponentially the detected probe intensity (as $\exp\left(\mathcal{A}_{\parallel}\right)$) but also amplifies *exponentially* the detected A^{cal}_{LR} asymmetry. In these measurements the probe intensity is fixed and two parameters are varied in order to change $\mathcal{A}$, the magnitude of $\boldsymbol{E}$ and the intensity of the excitation beam. As shown in Figure 3 the asymmetry depends only on $\mathcal{A}$ whichever parameter is varied. This

means that all ways of scaling-up $\mathcal{A}$ effectively result in a net gain as regards the $A_{\rm LR}$ amplification.

Experimental points in Figure 3 were obtained pairwise by switching the probe polarization between the configurations $\hat{\boldsymbol{\epsilon}}_{\rm pr}^{\rm in} \parallel \hat{\boldsymbol{\epsilon}}_{\rm ex}$ and $\hat{\boldsymbol{\epsilon}}_{\rm pr}^{\rm in} \perp \hat{\boldsymbol{\epsilon}}_{\rm ex}$. Dotted arrows show examples of such pairs. One can see that as long as the optical density is small, there is no advantage in working in the perpendicular configuration, since it appears that the smaller slope is compensated in the parallel case by a larger optical density. However, when the amplification is increased and $A_{\rm LR}^{\rm cal}/\theta^{\rm cal}$ *versus* $\mathcal{A}$ departs from a straight line, the advantage becomes conspicuous.

While $A_{\rm LR}$ is extracted from the differential signal, $S_{\rm X} - S_{\rm Y}$, which is free from any technical noise common to both channels, by contrast the optical density is evaluated from the sum signal, $S_{\rm X}+S_{\rm Y}$, and affected by a much larger noise. Therefore the dispersion among the experimental points of Figure 3 is essentially due to the experimental uncertainty on $\mathcal{A}$. As clearly shown by equation (10) this source of noise does not affect the determination of the PV angle which only involves the measurement of two differential signals, $A_{\rm LR}^{\rm pv}$ and $A_{\rm LR}^{\rm cal}$, performed in identical experimental conditions.

3.3 Absorption

The real situation is somewhat more complex because of a small isotropic background due to an atomic absorption $\mathcal{B} < 0$. The effectively measured amplification is : $\ln(I_{\rm pr}^{\rm out}/I_{\rm pr}^{\rm in}) = \mathcal{A} + \mathcal{B}$. Actually $\mathcal{B}$ is determined independently by tuning the excitation laser out of resonance. For the experimental data shown in Figure 3 the value of $\mathcal{B}$ varies between 0.05 ± 0.01 and 0.15 ± 0.02, its uncertainty affecting consequently the abscissae of the data points.

An important result of the theoretical calculations [21] was that the dependence of $A_{\rm LR}^{\rm cal}/\theta^{\rm cal}$ on the amplification parameter $\mathcal{A}$ is still conserved for realistic values of $\mathcal{B}$. The good match of $A_{\rm LR}^{\rm cal}/\theta^{\rm cal}$ with the theoretical curve confirms the overall theoretical predictions.

4 Gain of sensitivity due to $A_{\rm LR}$ amplification

4.1 Quantum noise in presence of amplification

The semi-classical treatment of the asymmetry amplification does not give any information about the quantum fluctuations of the amplified radiation field. However, if the input field is in a coherent state, it is well known that spontaneous emission introduces additional noise. In the particular case of linear amplification the variance of the photon number N of the amplified beam is given [25] by: $\sigma_N^2 = (2\exp(\mathcal{A}) - 1) < N >$. One can thus get the impression that the potential gain of sensitivity that was expected from the amplification of $A_{\rm LR}$ is made illusory because of the quantum fluctuations of the amplified beam. Nevertheless, a careful examination of this problem proves that this is not the case.

In fact the physical quantity that we must consider is not the total photon number N but rather the asymmetry $A_{\rm LR} = (S_{\rm Y} - S_{\rm X})/(S_{\rm Y} + S_{\rm X})$ which leads to the PV angle $\theta^{\rm pv}$ *via* equation (10). The signals $S_{\rm X}$ and $S_{\rm Y}$ are respectively proportional, with the same proportionality coefficient, to the photon numbers $N_{\rm X}$ and $N_{\rm Y}$ in the two channels detecting $\hat{\mathbf{X}}$– and $\hat{\mathbf{Y}}$–polarized light respectively. The variance of the L-R asymmetry is:

$$\sigma^2_{A_{\rm LR}} = \frac{< (\Delta N_{\rm Y} - \Delta N_{\rm X})^2 >}{(< N_{\rm Y} > + < N_{\rm X} >)^2} + A_{\rm LR}^2 \frac{< (\Delta N_{\rm Y} + \Delta N_{\rm X})^2 >}{(< N_{\rm Y} > + < N_{\rm X} >)^2} , \qquad (11)$$

where we shall treat the fluctuations of the photon number in each channel, $\Delta N_{\rm X}$ and $\Delta N_{\rm Y}$, to the lowest order. Since we are dealing with nearly balanced operation ($A_{\rm LR} \ll 1$) we write $< N_{\rm X} >=< N_{\rm Y} >=< N > / 2$ and we neglect the term involving $A_{\rm LR}^2$ in $\sigma^2_{A_{\rm LR}}$. We shall assume that at the same level of approximation , the amplified field state can be written as $|\Psi_\parallel > \otimes |0_\perp >$, where the index $\parallel$ and $\perp$ refer to the photons polarized along $(\hat{X}+\hat{Y})/\sqrt{2}$ and $(\hat{X}-\hat{Y})/\sqrt{2}$ and $|0_\perp >$ means a $\perp$–field in the vacuum state [26]. Without any other assumption concerning the statistical property of the field, explicit computations using the relations $a_{\rm X}^\dagger = (a_\parallel^\dagger + a_\perp^\dagger)/\sqrt{2}$ and $a_{\rm Y}^\dagger = (a_\parallel^\dagger - a_\perp^\dagger)/\sqrt{2}$ between the creation operators of the photons in the $\parallel$–, $\perp$–, X– and Y–polarized fields give:

$$< (\Delta N_{\rm X,Y})^2 > = < N_{\rm X,Y}^2 > - < N_{\rm X,Y} >^2 = \left(< (\Delta N)^2 > + < N >\right)/4 \quad (12)$$

$$< \Delta N_{\rm X}\, \Delta N_{\rm Y} > = \left(< (\Delta N)^2 > - < N >\right) 4. \quad (13)$$

Equation (13) shows a correlation between $N_{\rm X}$ and $N_{\rm Y}$ whenever the field state departs from a coherent state. As a result, the L-R asymmetry variance only involves the mean total number of detected photons and no other statistical property of the radiation field:

$$\sigma^2_{A_{\rm LR}} = \frac{1}{< N >} \cdot \qquad (14)$$

It is remarkable that the above mentioned deviation of the photon statistics with respect to Poisson's Law has no effect on $\sigma_{A_{\rm LR}}$, a property which is indeed used in the context of light detection at and below the shot noise limit (see *e.g.* [27,28]).

4.2 Quantum limited NEA

We can now estimate the sensitivity of the experiment to the electroweak asymmetry were it be limited only by quantum fluctuations. According to equation (10), since $\sigma_{A_{\rm LR}^{\rm pv}}/A_{\rm LR}^{\rm pv} \gg \sigma_{A_{\rm LR}^{\rm cal}}/A_{\rm LR}^{\rm cal}$, the standard deviation on $\theta^{\rm pv}$ is:

$$\sigma_{\theta^{\rm pv}} = \left(\frac{\theta^{\rm cal}}{A_{\rm LR}^{\rm cal}}\right) \sigma_{A_{\rm LR}^{\rm pv}}. \qquad (15)$$

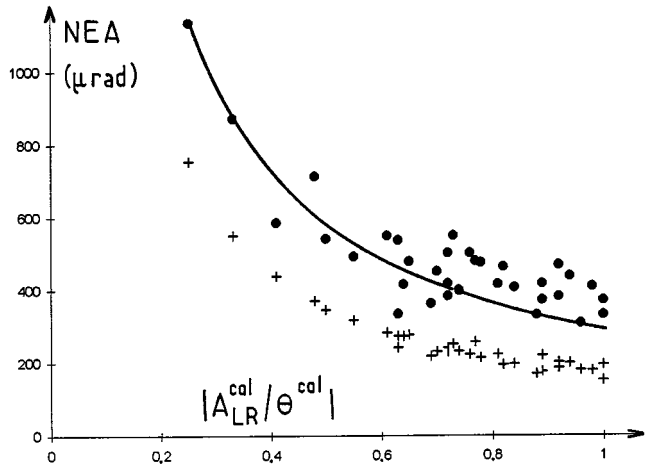

Fig. 4. NEA *vs.* $|A_{\rm LR}^{\rm cal}/\theta^{\rm cal}|$ for the $6S_{1/2}, F = 3 \rightarrow 7S_{1/2}, F = 4 \rightarrow 6P_{3/2}, F = 4$ transition and $\hat{\boldsymbol{\epsilon}}_{\rm pr}^{\rm in} \perp \hat{\boldsymbol{\epsilon}}_{\rm ex}$ (other conditions the same as in Fig. 3). Dots: observed NEA; solid line: expected $|A_{\rm LR}/\theta|^{-1}$ dependence; crosses: expected NEA (Eq. (16)) including shot-noise (calculated from the number of detected photoelectrons) and a small contribution to $\sigma_{A_{\rm LR}}$ from electronic noise.

The quantity $\sigma_{\theta^{\rm pv}}$ can be seen as a Noise Equivalent Angle (NEA):

$$\text{NEA} = \frac{1/\sqrt{N}}{A_{\rm LR}^{\rm cal}/\theta^{\rm cal}} \quad , \tag{16}$$

where N is the average number of detected photons. We thus expect any amplification of $A_{\rm LR}^{\rm cal}/\theta^{\rm cal}$ to result in a reduction of the NEA, *i.e.* a gain for the signal-to-noise.

4.3 Observed gain of sensitivity when $A_{\rm LR}$ is amplified

Figure 4 shows the measured NEA as a function of the L-R asymmetry amplification $A_{\rm LR}^{\rm cal}/\theta^{\rm cal}$ for the $6S_{1/2}, F = 3 \rightarrow 7S_{1/2}, F = 4 \rightarrow 6P_{3/2}, F = 4$ transition and $\hat{\boldsymbol{\epsilon}}_{\rm pr}^{\rm in} = \hat{\boldsymbol{\epsilon}}_{\parallel}$, at a fixed value of $I_{\rm pr}^{\rm in}$. Each point is the mean value of the NEA observed on an experimental run.

It is quite conspicuous that the NEA is reduced when the asymmetry amplification factor is increased. The general behaviour appears consistent with the inverse law dependence represented by the continuous curve, which indicates that the noise $\sigma_{A_{\rm LR}^{\rm pv}}$ is nearly constant. This means that no significant spurious noise is added by the amplification process, a fact which confirms the theoretical analysis of the previous paragraph. We note that we cannot expect to see the $1/\sqrt{N}$ reduction of $\sigma_{A_{\rm LR}^{\rm pv}}$ with amplification, the effect being too small in the optical density range explored.

However, a careful evaluation of the expected NEA (crosses in Fig. 4) shows the presence of some extra noise with respect to the expected quantum noise. The extra noise is responsible for the dispersion conspicuous on the observed noise. We are currently investigating different possible sources. Without excited atoms the observed noise is compatible with the shot noise limit. With excited atoms, we find that insertion of a Glan prism at the output of the Cs cell suppresses almost all the extra noise. A possible cause might come from inhomogeneities in the anisotropic optical components. Coupled to position jitter of the beams, for example due to turbulence near the hot cesium cell oven, they can generate genuine polarization noise. Perhaps also fluctuations in the geometry of the amplified probe beam coupling to imperfections of the analyzer can contribute to this extra noise [23].

Nevertheless, as the inset in Figure 3 shows, any further increase of $\mathcal{A}$ should continue to increase $|A_{\rm LR}^{\rm cal}/\theta^{\rm cal}|$ and thus improve the signal-to-noise ratio. Up to now, the best results are obtained for $\mathcal{A}_{\parallel}$ of the order of 0.45 yielding $|A_{\rm LR}^{\rm cal}/\theta^{\rm cal} \simeq 1.0|$ and $\sigma_{\theta^{\rm pv}} \approx 350$ μrad per laser shot.

5 Perspectives and conclusion

We have demonstrated the L-R asymmetry amplification with our PV experimental set-up. The observed exponential dependence in the optical density agrees with the theoretical study [21]. Noise measurements show that, although residual instrumental noise remains, the amplification process does not add noise by itself, and therefore a L-R asymmetry amplification effectively improves our sensitivity to $\theta^{\rm pv}$, a striking feature strongly associated with the use of balanced polarimetry. Consequently, all ways of scaling-up the optical density in our experiment deserve consideration. The parameter playing the most important role here is the gain anisotropy of the excited medium $(\alpha_{\parallel} - \alpha_{\perp})L$. If we refer to equation (1), we see that the main possibilities of improvements rely on the production of a *high density of* 7S *excited atoms*, but keeping also in mind the proportionality of α to $\gamma^{-1} = T_2$.

The density $\mathcal{N}_{7S}$ involves the ground state atomic density, the excitation cross-section, $\sigma_{\rm ex}$, itself proportional to E^2, and the number $n_{\rm ex}$ of excitation photons per pulse and per unit area: $\mathcal{N}_{7S} = \mathcal{N}_{6S}\ \sigma_{\rm ex}(E^2)\ n_{\rm ex}$. This emphasizes the importance of *boosting both the electric field, and the energy density* of the excitation beam. The experiment takes advantage also of the high atomic densities $\mathcal{N}_{6S}$ available in a saturated vapor. But above atomic densities of a few 10^{14} cm^{-3}, resonant collisions shorten T_2 as the inverse of the density, so that no further increase of α is expected at higher densities. However, one must remember that if we realize the condition $T_2 \ll t_{\rm p}$, instead of $T_2 = 0.7\ t_{\rm p}$ in the present situation, then the optical thickness $\mathcal{A}$ *versus* the amplification parameter, αL, acquires a larger slope: 2.0 instead of 0.6. This suggests operating the experiment at larger atomic densities. Another important prediction of the theory [21] is that an increase of the probe intensity further improves the NEA since it should conserve the $A_{\rm LR}/\theta$ amplification factor of the $6S_{1/2,F\pm1} \rightarrow 7S_{1/2,F} \rightarrow 6P_{3/2,F}$ hfs transitions and decrease the quantum noise $1/\sqrt{< N >}$. This has also been checked by operating our current probe laser at the largest available intensities. A new diode laser system is under construction to reach a much higher intensity.

In conclusion, our PV experiment bears new interesting features with respect to former ones in its use of an optical amplification process in a strongly anisotropic medium and balanced polarimetry, two techniques unusual in this domain of physics.

References

1. M.A. Bouchiat, C. Bouchiat, Phys. Lett. **B 48**, 111 (1974).
2. M.A. Bouchiat, J. Guéna, L. Hunter, L. Pottier, Phys. Lett. **B 117**, 358 (1982).
3. M.A. Bouchiat, J. Guéna, L. Hunter, L. Pottier, Phys. Lett. **B 134**, 463 (1984).
4. M. Davier, J. Phys. France **43**, C3, 471 (1982).
5. C.S. Wood, S.C. Bennett, D. Cho, B.P. Masterson, J.L. Roberts, C.E. Tanner, C.E. Wieman, Science **275**, 1759 (1997).
6. V.A. Dzuba, V.V. Flambaum, O.P. Sushkov, Phys. Lett. **1141**, 147 (1989).
7. S.A. Blundell, W.R. Johnson, J. Sapirstein, Phys. Rev. Lett. **65**, 1411 (1990).
8. S.A. Blundell, J. Sapirstein, W.R. Johnson, Phys. Rev. **D45**, 1602 (1992).
9. C. Adloff *et al.*, Z. Phys. **C 74**, 191 (1997); J. Breitweg *et al.*, Z. Phys. **C 74**, 207 (1997).
10. A.E. Nelson, Phys. Rev. Lett. **78**, 4159 (1997).
11. M.C. Noecker, B.P. Masterson, C.E. Wieman, Phys. Rev. Lett. **61**, 310 (1988).
12. P.S. Drell, E.D. Commins, Phys. Rev. Lett. **53**, 968 (1984).
13. M.J.D. Macpherson, K.P. Zetie, R.B. Warrington, D.N. Stacey, J.P. Hoare, Phys. Rev. Lett. **67**, 2784 (1991).
14. R.B. Warrington, C.D. Thompson, D.N. Stacey, Europhys. Lett. **24**, 641 (1993).
15. D.M. Meekhof, P. Vetter, P.K. Majumder, S.K. Lamoreaux, E. Fortson, Phys. Rev. Lett. **71**, 3442 (1993).
16. N.H. Edwards, S.J. Phipp, P.E.G. Baird, S. Nakayama, Phys. Rev. Lett. **74**, 2654 (1995).
17. P. Vetter, D.M. Meekhof, P.K. Majumder, S.K. Lamoreaux, E. Fortson, Phys. Rev. Lett. **74**, 2658 (1995).
18. M.A. Bouchiat, C. Bouchiat, J. Phys. France **36**, 493 (1975).
19. M.A. Bouchiat, Ph. Jacquier, M. Lintz, L. Pottier, Optics Comm. **56**, 100 (1985).
20. M.A. Bouchiat, J. Guéna, M. Lintz, L. Pottier , Optics Comm. **77**, 374 (1990).
21. C. Bouchiat, M.A. Bouchiat, Z. Phys. **D 36**, 105 (1996).
22. J. Guéna, Ph. Jacquier, M. Lintz, L. Pottier, M.A. Bouchiat, Optics Comm. **71**, 6 (1989).
23. M.A. Bouchiat, D. Chauvat, J. Guéna, Ph. Jacquier, M. Lintz, M.D. Plimmer, Optics Comm. **119**, 403 (1995).
24. J. Guéna, D. Chauvat, Ph. Jacquier, M. Lintz, M.D. Plimmer, M.A. Bouchiat, J. Opt. Soc. Am. **B 14**, 271 (1997).
25. L. Mandel, E. Wolf, *Optical Coherence and Quantum Optics* (Cambridge University Press, Cambridge, 1995).
26. This not so trivial approximation will be discussed in a more general context in a forthcoming paper on quantum fluctuations in balanced polarimetry.
27. P. Grangier, R.E. Slusher, B. Yurke, A. LaPorta, Phys. Rev. Lett **59**, 2153 (1987).
28. J. Mertz, A. Heidmann, C. Fabre, E. Giacobino, S. Reynaud, Phys. Rev. Lett **64**, 2897 (1990).